Systems/Circuits

Hypocretin/Orexin Interactions with Norepinephrine Contribute to the Opiate Withdrawal Syndrome

Ronald McGregor,[1,2] Ming-Fung Wu,[1,2] Brent Holmes,[2,4] Hoa Anh Lam,[1,8] Nigel T. Maidment,[1,3,8] Joseph Gera,[2,4,5,6] Akihiro Yamanaka,[7] and Jerome M. Siegel[1,2,3]

[1]Department of Psychiatry and Biobehavioral Sciences, University of California, Los Angeles, Los Angeles, California 90095, [2]Veterans Administration Greater Los Angeles Healthcare System, North Hills, Los Angeles, California 91343, [3]Brain Research Institute, University of California, Los Angeles, Los Angeles, California 90095, [4]Department of Medicine, University of California, Los Angeles, Los Angeles, 90095, [5]Jonnson Comprehensive Cancer Center, University of California, Los Angeles, Los Angeles, 90095, [6]Molecular Biology Institute, University of California, Los Angeles, Los Angeles, 90095, [7]Department of Neuroscience II, Research Institute of Environmental Medicine, Nagoya University, Nagoya 464-8601, Japan, and [8]Hatos Center for Neuropharmacology, University of California, Los Angeles, Los Angeles, California 90095

We previously found that human heroin addicts and mice chronically exposed to morphine exhibit a significant increase in the number of detected hypocretin/orexin (Hcrt)-producing neurons. However, it remains unknown how this increase affects target areas of the hypocretin system involved in opioid withdrawal, including norepinephrine containing structures locus coeruleus (LC) and A1/A2 medullary regions. Using a combination of immunohistochemical, biochemical, imaging, and behavioral techniques, we now show that the increase in detected hypocretin cell number translates into a significant increase in hypocretin innervation and tyrosine hydroxylase (TH) levels in the LC without affecting norepinephrine-containing neuronal cell number. We show that the increase in TH is completely dependent on Hcrt innervation. The A1/A2 regions were unaffected by morphine treatment. Manipulation of the Hcrt system may affect opioid addiction and withdrawal.

Key words: **addiction; anatomy; hypocretin; locus coeruleus; opioids; withdrawal**

Significance Statement

Previously, we have shown that the hypothalamic hypocretin system undergoes profound anatomic changes in human heroin addicts and in mice exposed to morphine, suggesting a role of this system in the development of addictive behaviors. The locus coeruleus plays a key role in opioid addiction. Here we report that the hypothalamic hypocretin innervation of the locus coeruleus increases dramatically with morphine administration to mice. This increase is correlated with a massive increase in tyrosine hydroxylase expression in locus coeruleus. Elimination of hypocretin neurons prevents the tyrosine hydroxylase increase in locus coeruleus and dampens the somatic and affective components of opioid withdrawal.

Introduction

We (Mileykovskiy et al., 2005; McGregor et al., 2011; Wu et al., 2011a,b; Blouin et al., 2013) and others (Nestler et al., 2002; Georgescu et al., 2003; Harris et al., 2005; Boutrel and de Lecea, 2008; Borgland et al., 2009; Aston-Jones et al., 2010; Nestler, 2013; Baimel et al., 2015; James et al., 2017) have shown that hypocretins/orexins (Hcrts) play a key role in processing rewards. Recently, we reported that the number of detectable Hcrt neurons is greatly increased in human heroin addicts as well as in mice administered daily injections of morphine for 2 weeks (Thannickal et al., 2018; Donjacour et al., 2019). It was then shown that chronic exposure to cocaine produced a similar increase in the number of detected Hcrt neurons in rats (James et al., 2019). These findings suggest a major role of Hcrt plasticity in the addictive process. However, it remains unknown how target areas of the Hcrt system that are critically related to opioid addiction, including norepinephrine (NE) containing locus coeruleus (LC) and the NE-containing A1/A2 medullary nuclei (Christie et al., 1997; Peyron et al., 1998; Delfs et al., 2000; Blanco-Centurion et al., 2007; Sharf et al., 2008; Valentino and Van Bockstaele, 2008; Mazei-Robison and Nestler, 2012; Parkitna et al., 2012; Chaijale et al., 2013; Jaremko et al., 2014; Kaeidi et al., 2015; Zhang et al., 2017; Solecki et al., 2019), are affected by the increase in the number of detected Hcrt neuronal

Received July 30, 2021; revised Sep. 21, 2021; accepted Oct. 9, 2021.

Author contributions: R.M., M.-F.Wu, N.T.M., J.G., and J.M.S. designed research; R.M., M.-F.W., B.H., and H.A.L. performed research; A.Y. contributed unpublished reagents/analytic tools; R.M., M.-F.W., B.H., H.A.L., N.T.M., and J.M.S. analyzed data; R.M., N.T.M., J.G., B.H., M.-F.W., H.A.L., and J.M.S. wrote the paper.

J.M.S. was supported by Department of Health and Human Services (HHS) | National Institutes of Health (NIH) | National Institute on Drug Abuse (NIDA) Grant DA-034748; N.T.M. was supported by HHS | NIH | NIDA Grants P50DA005010, DA-034748, AG-063090, and UG3-TR-003148; and J.G. was supported by Medical Research Service of the VA Grants CA217820 and I01BX002665.

The authors declare no competing financial interests.

Correspondence should be addressed to Ronald McGregor at icelos3@gmail.com.

https://doi.org/10.1523/JNEUROSCI.1557-21.2021

somas. We now find that chronic morphine administration greatly increases Hcrt projections to the LC. In contrast no increase is seen in the A1/A2 areas. Morphine treatment greatly increases tyrosine hydroxylase (TH) expression in LC. We find that this increase is completely dependent on Hcrt innervation. Hcrt removal did not affect acquisition of morphine conditioned place preference (CPP) but prevented locomotor sensitization to repeated drug administration. Hcrt depletion significantly reduced the physical withdrawal symptoms induced by naloxone and the aversion to a chamber associated with naloxone in morphine-dependent animals. These findings may explain the minimal drug withdrawal effects and the low rate of drug addiction seen in narcoleptic humans, a disease caused by the loss of Hcrt neurons. They also support a role for Hcrt antagonists in treating opiate addiction.

Materials and Methods

Subjects

Animal usage. All procedures were approved by the Institutional Animal Care and Use Committees of the University of California, Los Angeles, and of the Veterans Administration Greater Los Angeles Health Care System.

Animals. Experiments were performed in genetically modified C57BL/6 mice expressing diphtheria toxin fragment A (DTA) exclusively in Hcrt neurons (DTA-Hcrt) under the control of the Tet-Off system. In these animals, postnatal ablation of Hcrt neurons can be induced by doxycycline withdrawal, as previously described (John et al., 2013; Tabuchi et al., 2014). Complete ablation of Hcrt neurons was accomplished in one group of animals (depleted-DTA-Hcrt) by removing doxycycline from the diet for 30 d beginning at 42 d of age, after which doxycycline-containing feed was resumed. Control animals (intact-DTA-Hcrt) were maintained throughout the study on the diet containing doxycycline. A total of 140 male mice were used in the current study (Table 1 shows the number of animals in each experiment). All experimental procedures were started when animals reached 3 months of age. Animals were kept in a room maintained at 22 ± 1°C on a 12 h light (45 lux)/dark (0.03 lux) cycle, with lights on at 7:00 A.M. [zeitgeber time 0 (ZT0)] and lights off at 7:00 P.M. (ZT12).

Drugs

Morphine (morphine sulfate, Hospira) and naloxone (naloxone hydrochloride dihydrate; catalog #N7758, Millipore Sigma) were used. Morphine and naloxone were dissolved in sterile saline immediately before subcutaneous administration.

Behavioral studies

Sensitization to morphine. Locomotor activity was monitored using digital video recordings. Briefly, cameras (Analog HD 1080p, LBV2723, Lorex Technology, Canada) were suspended above modified laboratory cages (40 × 20 × 50 cm). Animals were placed in the cages and allowed 14 d of acclimation under continuous video recording. After this initial period, morphine (50 mg/kg, s.c.) or saline (subcutaneous) was administered for 14 d at ZT2 to intact-DTA-Hcrt and depleted-DTA-Hcrt mice. A 30 min video started immediately after the injection and was analyzed using open-source automated rodent tracker software (Hewitt et al., 2018) to quantify locomotor activity.

Conditioned place preference. The CPP test was conducted in a Plexiglas shuttle box composed of two compartments of equal size (18 × 12.5 × 12.5 cm) separated by a sliding door (model MED-CPP2-MS, Med Associates). One side had white walls and a mesh floor. The other had black walls and a grid rod floor. We used a biased design approach in which the preference of each individual subject for a particular environment before conditioning was assessed first by placing the animals in the apparatus for 15 min on 3 consecutive days, and quantifying the time spent in each compartment. The less preferred compartment for each subject was then assigned as the drug-paired compartment.

Table 1. Number of animals used in each experimental procedure

Experiment	Animals, *n*
LC quantification of immunofluorescence	16
LC quantification of TH cell number	12
A1/A2 quantification of immunofluorescence	12
A1/A2 quantification of TH cell number	8
Western blots	12
Conditioned place preference	24
Sensitization	12
Withdrawal from escalating vs fixed morphine dose	12
Naloxone-precipitated withdrawal	12
Naloxone aversion	20

The table depicts the number of animals used for each experimental procedure.

On days 1, 2, and 3, each mouse was placed in either the white or the black compartment, alternating each day, with the door open for 15 min. The amount of time the animal spent in either chamber was recorded. On the subsequent 6 d, place preference conditioning was conducted using a counterbalanced design. On days 4, 6, and 8, mice received either a saline (2 ml/kg, s.c.) or a morphine (5 mg/kg, s.c.) injection and were confined to one of the conditioning chambers for 30 min. On days 5, 7, and 9, mice received the opposite treatment and were confined to the opposite chamber. The postconditioning testing (day 10) consisted of placing the animal in the saline-conditioned compartment and allowing it free access to both chambers for 15 min. The difference in time spent in the morphine-paired chamber between testing and baseline periods was calculated (CPP score; Sharf et al., 2010). This design does not elicit anxiety-like behaviors in response to morphine (Benturquia et al., 2007; Prus et al., 2009).

Precipitated withdrawal. Intact-DTA-Hcrt and depleted-DTA-Hcrt mice were made morphine dependent by being given either a 14 d, once per day (ZT3), dose of morphine (50 mg/kg, s.c.) or a 5 d escalating dose of morphine, administering the drug twice a day at ZT3 and ZT8 in the following schedule: day 1, 20 and 40 mg/kg; day 2, 40 and 60 mg/kg; day 3, 60 and 80 mg/kg; day 4, 80 and 100 mg/kg; day 5, single dose (ZT3) 100 mg/kg. Two hours after the last morphine injection, naloxone (2 mg/kg, s.c.) was administered and behavioral withdrawal symptoms were assessed. This experiment was performed to establish whether our single fixed daily dose of morphine injection for 14 d generates comparable somatic signs of opioid withdrawal to escalating morphine doses (see Results). All sessions were conducted in Plexiglas cages. We quantified locomotion, jumping, backward stepping, rearing, paw tremor, teeth chattering, grooming, behavioral arrest, defecation, urination, wet dog shake, ptosis, diarrhea, body tremor, and piloerection. A global withdrawal score was calculated (Maldonado et al., 1996; Georgescu et al., 2003; Sharf et al., 2008; Zhang et al., 2016). Two hours after naloxone administration, animals were killed and processed for immunohistochemistry (see below).

Naloxone conditioned place aversion. Place conditioning took place in square chambers (26 × 26 × 19.5 cm) with infrared photobeam sensors that allowed for automated recording of subject location (time spent in each chamber) and locomotor activity (TruScan, Coulbourn Instruments). The chambers were divided into two smaller chambers of equal size (26 × 13 × 19.5 cm) by a Plexiglas partition. One of these chambers contained white walls with black dots (diameter, 1.5 cm), a dark metal floor with large punched circles (diameter, 0.5 cm), and 20 µl of lemon liquid extract (McCormick) placed on a slip of paper taped to the top of the chamber. The other chamber contained blue walls, a silver metal floor with small punched circles (diameter, 0.3 cm), and 120 µl of almond liquid extract (McCormick) placed on a slip of paper taped to the top of the chamber. For the 15 min preconditioning and postconditioning test sessions, the center divider was replaced with a similar divider that incorporated a small opening in the bottom (5 × 5 cm). At the start of all conditioning and testing sessions, animals were placed directly into the front left corner of the predetermined chamber. A computer running TruScan software controlled all experimental events and recorded behavioral data.

Drug treatment and conditioning. On days 1–5, mice received a single daily injection of escalating doses of morphine in the home cage (ZT3: 10, 20, 30, 40, 50 mg/kg, s.c.). On day 6, 20 h after the last morphine injection (50 mg/kg, s.c.), mice were injected with saline and immediately placed in one of the two chambers (saline-paired chamber) for 30 min. Upon returning to their home cages, animals received a subsequent dose of morphine (50 mg/kg, s.c.). On day 7, 20 h after the morphine injection, animals received either 0.05 or 0.2 mg/kg (s.c.) naloxone and were immediately placed in the alternate side of the chamber (naloxone-paired chamber) for 30 min. Upon return to their home cages, animals received another dose of morphine (50 mg/kg, s.c.). This conditioning procedure was repeated on consecutive days in an alternating fashion such that each animal was exposed to 3 d of saline and 3 d of naloxone conditioning. On the subsequent test day, 20 h after the final morphine dose, animals were allowed free access to both chambers for 15 min and the time spent in each chamber was recorded.

For this experiment, an unbiased design was used, with assignment of saline- and naloxone-paired chambers being made on the basis of pretest conditioning data to ensure a balance between time spent in future saline-paired versus future naloxone-paired chambers within and across groups. An aversion score was calculated by subtracting the time spent in the naloxone-paired chamber from time spent in the saline-paired chamber during the postconditioning test.

Western blot. All animals were killed between ZT5 and ZT7. Animals were deeply anesthetized with pentobarbital (Nembutal, 100 mg/kg, i.p.) and decapitated. Brains were quickly removed from the skull, and the locus coeruleus was dissected. Tissue was then sonicated in lysis buffer containing 50 mM Tris HCl, 50 mM MgCl2, 5 mM EDTA, and protease inhibitor tablet (catalog #12482000, Roche); and centrifuged at 800 × *g* (3000 rpm) for 30 min at 4°C. The protein concentration of the supernatant was determined using the DC Protein Assay Kit (catalog #500–0112, BIO-RAD). Forty micrograms of protein was loaded on a 12% Mini-PROTEAN TGX Precast Gel (catalog #456–1044, BIO-RAD), and separated at 50 V. The proteins were then transferred to a PVDF membrane (catalog #162–0176, BIO-RAD) at 50 mA for 120 min. The membrane was washed in 20 mM Tris, 150 mM NaCl, and 0.1% Tween 20 (TBST), and then blocked in TBST containing 5% (w/v) nonfat dry milk (NFDM) for 60 min. The membrane was incubated with rabbit anti-TH antibody (1:1000; catalog #2792, lot #6, Cell Signaling Technology) in 5% NFDM in TBST overnight at 4°C. The next day, the membrane was washed in TBST before incubation with donkey anti-rabbit HRP-conjugated secondary antibody (1:10,000; catalog #NA934V, lot #16963367, GE Healthcare Life Sciences) at a dilution of in 5% NFDM in TBST, for 60 min at room temperature. After washing in TBST, the antibody complex was visualized with SuperSignal West Femto (catalog #34094, Thermo Fisher Scientific). Anti-β-actin (1:10,000; catalog #A2228, lot #099M4776V, Sigma-Aldrich) was used as an internal normalizer, with sheep anti-mouse HRP-conjugated secondary antibody (1:10,000; catalog #NA913V, lot #16814909, GE Healthcare Life Sciences). The densities of TH and β-actin bands for each sample were measured using ImageJ software.

Anatomical studies

Tissue processing. All animals were killed between ZT5 and ZT7. For tissue collection, animals were deeply anesthetized with pentobarbital (Nembutal, 100 mg/kg, i.p.) and transcardially perfused with 0.035 L of heparinized (1000 U/L) PBS, 0.1 M, pH 7.4, followed by 0.07 l of 4% paraformaldehyde in phosphate buffer, 0.1 M, pH 7.4. Brains were removed and coded. All subsequent procedures were performed by an investigator blind to the procedures performed before killing. Brains were immersed in PBS with 20% sucrose and then transferred to 30% sucrose solution for cryoprotection.

Forty-eight hours later, each brain was frozen and cut into 40 μm coronal sections using a sliding microtome (American Optical). Each section was placed in one well of a three-well tray containing PBS, and immunohistochemical procedures were performed immediately. The remaining tissue was transferred to a cryoprotectant solution and stored at −20°C.

Immunohistochemistry. All immunohistochemical procedures were performed on free-floating sections. The sections were incubated in both primary antibodies overnight at room temperature in PBS with 0.25% Triton X-100 (PBST), followed by incubation (PBST) in the corresponding secondary antibody tagged with fluorophores that match our microscope filters (Alexa Fluor, Thermo Fisher Scientific) with lights off and samples wrapped in aluminum foil. Tissue was mounted and coverslipped using VECTASHIELD Antifade Mounting Media (catalog #H1000, lot #2E00806, Vector Laboratories). For identification of NE-containing neurons in the LC and A1/A2 medullary regions, we used the immunohistochemical detection of TH enzyme. To quantify the number of NE neurons, the same mounting media containing DAPI was used (catalog #H1200, lot #2E0815, Vector Laboratories).

The following antibodies were used: for Hcrt-1, rabbit anti-Hcrt-1 (1:2000; catalog #H-003–36, lot #01651–1, Phoenix Pharmaceuticals); and for TH, sheep anti-TH (1:1000; catalog #ab-113, lot # GR3277795-16, Abcam).

All tissue sections from experimental and control animals were stained at the same time and with the same antibody lot.

Data collection

The number and distribution of Hcrt fibers and TH cell bodies was assessed using a confocal microscope (model LSM 900 with Imager Z2 AX10 software, Zeiss) equipped with the appropriate lasers. Every section that contained the LC and the A1/A2 regions was imaged at 1 µm optical planes; 27 ± 1.2 optical planes were obtained per section. Quantification was performed bilaterally. Immunofluorescence intensities and area measurements were obtained using Zeiss proprietary software (ZEN). The area was defined by the size of the region containing TH^+ neuronal bodies in each structure. Total immunofluorescence for TH and Hcrt was divided by the corresponding area, and bilateral areas in the same section were averaged. Cell number and fiber distribution were determined using Adobe Illustrator. Every stack of images was loaded in this program such that each optical plane was placed in a distinct layer and individual TH^+ neurons were identified and marked. Using this method of quantification eliminates double counting of cells, which is critical in the analysis of structures with a high density of neuronal bodies like the LC. For the analysis of Hcrt fiber distribution, the middle optical plane was chosen for sections that contained the densest TH^+ neuronal bodies distribution within the LC. Individual fibers were drawn and measured, and the fiber density was calculated based on the same area used to calculate the immunofluorescence intensities. To further explore the distribution of Hcrt fibers within the LC, we divided the structure into a dorsal and a ventral portion by placing a straight line across the middle of the LC and perpendicular to the dorsoventral axis. In a second set of analyses we divided the LC into a medial and lateral portion (defined in reference to the fourth ventricle; medial portion = proximal to the fourth ventricle) by placing a straight line from the apex of the structure to the middle of the inferior limit of the LC.

Statistical analysis

Data were subjected to either ANOVA followed by Tukey's *post hoc* test comparisons, or *t* test. All such tests were two tailed. Results were considered statistically significant at $p < 0.05$. The number of subjects in each experimental procedure is indicated by degrees of freedom.

Results

Anatomy

Morphine treatment increases Hcrt axonal labeling in the LC

We observed a significant increase of 52.3% in Hcrt staining in the LC of animals injected with morphine, compared with animals injected with saline (Fig. 1*a*; $p = 0.022$, df = 6, *t* test). This increase in immunofluorescence intensity was linked to a significant increase (201.4%) in the number of Hcrt-immunopositive fibers per unit of area (Hcrt fiber density) in the LC (Fig. 1*b*; $p = 0.0044$, df = 6, *t* test). The difference was visually apparent, as

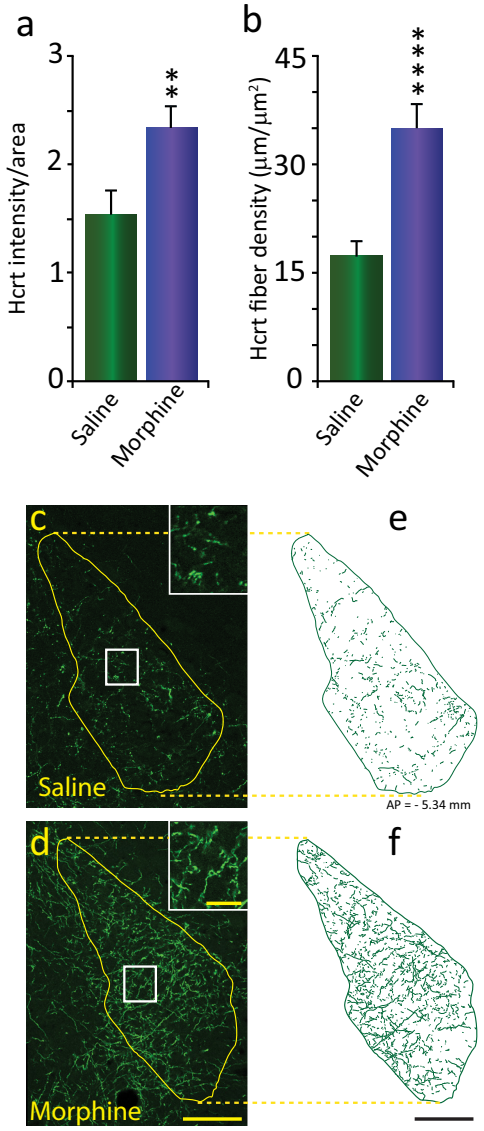

Figure 1. Morphine treatment increases Hcrt axonal labeling in the locus coeruleus. ***a***, Morphine treatment (once a day, 14 d, 50 mg/kg, s.c.) resulted in a significant increase of Hcrt immunofluorescence intensity per unit of area (52.3%) compared with saline treatment in the LC of intact-DTA-Hcrt animals. All error bars in the figures are the SEM. ***b***, This was the result of a significant increase (201.4%) in the density of Hcrt axons. ***c***, ***d***, Confocal images of representative sections of Hcrt axons in the LC of intact-DTA-Hcrt animals after saline (***c***) or morphine (***d***) treatment. The difference in Hcrt innervation is visually apparent. Inserts in ***c*** and ***d*** show higher magnifications of the square area, shown in white. ***e***, ***f***, Hcrt fiber tracings of the LC in a saline-treated (***e***) or morphine-treated (***f***) intact-DTA-Hcrt animal. The confocal images of the LC were obtained from the same section double stained for Hcrt and TH (Fig 2*e*, saline and morphine). Scale bars: 100 μm; insert, 20 μm. $^{****}p = 0.004$, $^{**}p = 0.022$. $n = 4$/condition.

seen in the confocal images in Figure 1, *c* (saline) and *d* (morphine), taken at the same anterior-posterior level. Inserts show the area outlined within the white square at higher magnification, illustrating the increase in fiber density. Figure 1, *e* and *f*, show fiber tracings of the circumscribed area outlined in yellow for each condition (scale bars: yellow, 100 μm; insert, 20 μm; black, 100 μm). We did not observe a significant difference in the distribution of Hcrt fiber density between the LC areas analyzed under the saline condition (dorsal, 6.87 ± 0.64; vs lateral, 8.12 ± 0.94; $p = 0.316$, df = 6, *t* test; lateral, 7.88 ± 0.47; vs medial, 7.61 ± 0.81; $p = 0.78$, df = 6, *t* test) or after morphine (dorsal, 14.15 ± 1.03; vs lateral, 15.95 ± 1.06; $p = 0.269$, df = 6, *t* test; lateral, 14.54 ± 1.05; vs medial, 15.54 ± 0.7; $p = 0.46$, df = 6, *t* test).

Morphine treatment increases TH levels and immunofluorescence intensity in the LC without increasing the number of labeled cells, dependent on Hcrt innervation

We observed a significant increase (69.9%) in the levels of TH in the LC, as illustrated in the Western blot assay shown in Figure 2, *a* (top) and *b* ($p = 0.035$, df = 10, *t* test). Cytoskeletal β-actin protein was unaffected by morphine treatment (Fig. 2*a*, bottom). This change was associated with a significant (80.1%) increase in the intensity of TH immunofluorescence in LC after morphine treatment (Fig. 2*c*; $p = 0.029$, df = 6, *t* test), establishing a relation between TH levels and TH immunofluorescence intensity. The increase in TH levels detected in the LC after morphine treatment was not the result of an increase in the number of TH-expressing neurons in this structure (Fig. 2*d*). Rather, individual neurons showed a higher concentration of the enzyme, as illustrated in the confocal images (Fig. 2*e*) of representative sections of the LC in an animal treated with saline (Fig. 2*e*, left) and morphine (Fig. 2*e*, middle). When Hcrt innervation was eliminated (depleted-DTA-Hcrt) before the 2 week daily injection of 50 mg/kg morphine, there was no difference in the TH immunofluorescence intensity between morphine-treated animals and saline controls (Fig. 2*e*, right, *f*) indicating that Hcrt neurons are necessary for the morphine-induced increase in LC TH levels (Fig. 2*e*, *f*, scale bar, 100 μm). Lack of Hcrt did not affect the number of TH^+ neurons after morphine treatment compared with saline- and morphine-treated animals (Fig. 2*g*).

Morphine treatment does not alter Hcrt axon density or TH levels in the A1/A2 medullary norepinephrine-containing regions

It has been proposed that medullary NE cell groups A1 and A2, acting through their projections to the ventral bed nucleus of the stria terminalis, are critical in withdrawal behavior, rather than LC (Delfs et al., 2000; Fox et al., 2016). In the current study, we found that Hcrt innervation and TH levels of the A1 and A2 medullary NE nuclei were unaffected by morphine treatment (Fig. 3*a–d*) in mice in which the Hcrt system was intact (intact-DTA-Hcrt). Furthermore, deletion of Hcrt neurons did not affect the number of TH^+ neurons in the A1 or A2 regions (Fig. 3*e*,*f*). Depleted-DTA-Hcrt mice treated with morphine did not show significant changes to the TH levels in either of these medullary NE regions compared with animals with the full contingent of Hcrt neurons (intact-DTA-Hcrt mice) treated with saline or morphine (Fig. 3*g*,*h*). Representative examples of low-magnification confocal images of the A1 (Fig. 3*i*) and A2 (Fig. 3*j*) medullary regions of an intact-DTA-Hcrt animal treated with saline showing the distribution of TH^+ cell bodies in red (yellow arrows) and Hcrt fibers in green (white arrowheads). The insert in Figure 3*j* shows a higher magnification of the white rectangle (scale bars: 100 μm; insert, 20 μm).

Behavior

The rewarding properties of morphine as measured herein are not significantly affected by the lack of Hcrt neurons. But Hcrt depletion prevents locomotor sensitization and reduces both the somatic signs of naloxone-precipitated withdrawal and naloxone conditioned place aversion (CPA) in morphine-dependent animals.

Intact-DTA-Hcrt and depleted-DTA-Hcrt animals both developed CPP to morphine (Fig. 4*a*). However, locomotor sensitization to repeated drug administration was significantly

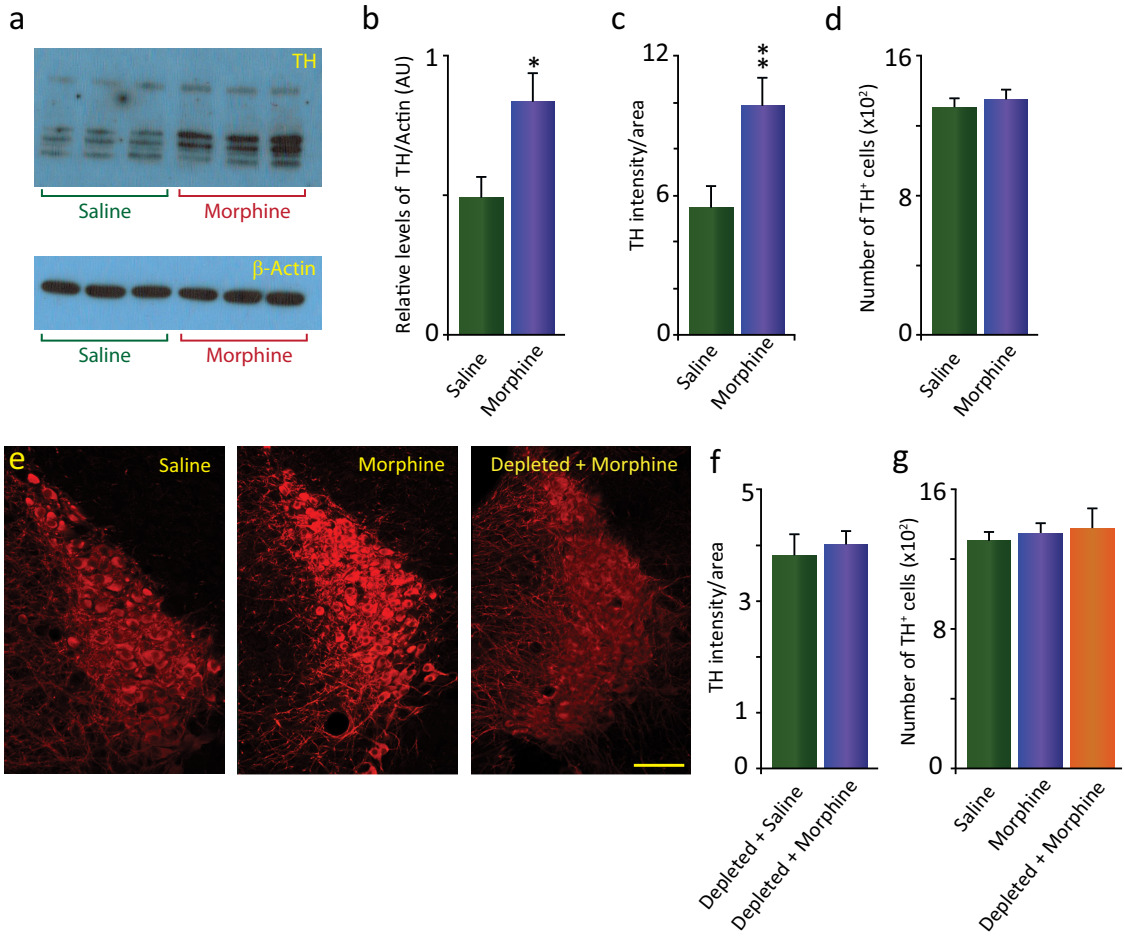

Figure 2. Morphine treatment increases TH immunofluorescence intensity in the LC without increasing the number of labeled cells. This effect is dependent on Hcrt innervation. ***a***, Top, Western blot assay showing a significant increase (69.9%) in the levels of TH in intact-DTA-Hcrt animals treated with morphine (14 d, 50 mg/kg, s.c.) compared with saline animals (left, saline; right, morphine; $n = 6$/condition). Bottom, β-Actin control. ***b***, Relative density of bands expressed as the ratio of TH and β-actin in animal groups. ***c***, Elevation of TH levels was reflected in a significant increase in the TH immunofluorescence intensity per unit of area (80.1%) compared with saline in the LC ($n = 4$/condition). ***d***, No significant difference in the number of TH-expressing cells in the LC in animals treated with morphine compared with saline was observed ($n = 4$/condition). ***e***, Confocal images of representative sections of the LC of intact-DTA-Hcrt animals after saline (left) or morphine (middle) treatment. The difference in TH immunofluorescence is visually recognizable. When Hcrt neurons were depleted (right), there was no difference in TH immunofluorescence between animals injected with morphine and animals injected with saline ($n = 4$/condition). ***f***, Group data showing no significant difference in TH labeling in depleted-DTA-Hcrt mice given saline and depleted-DTA-Hcrt mice given 14 d of 50 mg/kg morphine. ***g***, There is no significant difference in the number of TH-expressing cells in the LC of mice lacking Hcrt neurons and treated with morphine compared with intact animals treated with saline or morphine ($n = 4$/condition). Scale bar, 100 μm. $^{**}p = 0.029$, $^{*}p = 0.035$.

affected by Hcrt condition (depleted vs intact: $F_{(1,20)} = 4.53$, $p = 0.046$, df = 1, 20), 14 d of morphine injection ($F_{(1,20)} = 8.45$, $p = 0.009$, df = 1, 20), and Hcrt condition by days of morphine injection interaction ($F_{(1,20)} = 6.82$, $p = 0.017$, df = 1, 20). A Tukey's *post hoc* comparison showed that there was a significant increase in locomotion in intact-DTA-Hcrt animals after 14 d of morphine administration compared with day 1 (Fig. 4*b*, $p = 0.04$). Depleted-DTA-Hcrt animals did not show this locomotor sensitization (Fig. 4*c*).

Escalating morphine doses have been previously used to assess the somatic signs of precipitated opioid withdrawal. In this study, we determined that our 14 d regimen of daily injection of a fixed dose of morphine (Thannickal et al., 2018) resulted in a global withdrawal score similar to that of the escalating morphine schedule (Fig. 4*d*). Depleted-DTA-Hcrt animals showed a significant decrease in the global withdrawal score compared with intact-DTA-Hcrt animals after naloxone-precipitated withdrawal (Fig. 4*e*; $p = 0.043$, df = 10, *t* test). Paw tremor and rearing were greatly reduced during withdrawal in depleted-DTA-Hcrt animals compared with intact-DTA-Hcrt animals (Fig. 4*f*: $p = 0.007$, df = 10; Fig. 4*g*: $p = 0.0001$, df = 10; *t* tests). In addition, morphine-treated depleted-DTA-Hcrt animals displayed significantly less aversion to the chamber paired with naloxone at the higher of the two doses (0.05 and 0.2 mg/kg) tested in the CPA test (a dose that did not induce physical withdrawal symptoms), indicating a reduction in the affective component of morphine withdrawal (Fig. 4*h*: $p = 0.002$, df = 18, *t* test). The lower naloxone dose produced minimal aversion, and there was no difference between Hcrt depleted and intact (data not shown).

Discussion

We have reported that the brains of human heroin addicts and of mice exposed to opioids present a substantially higher number of Hcrt-immunopositive neurons compared with controls (Thannickal et al., 2018). We speculate that the elevation of Hcrt levels may result from the excitatory effects of morphine on Hcrt neurons *in vivo* that we previously reported (Thannickal et al., 2018). We now show that this hypothalamic anatomic change induced by morphine also produces a significant increase in the Hcrt axonal presence in the LC, a NE-containing structure involved in the modulation of opioid withdrawal (Christie et al.,

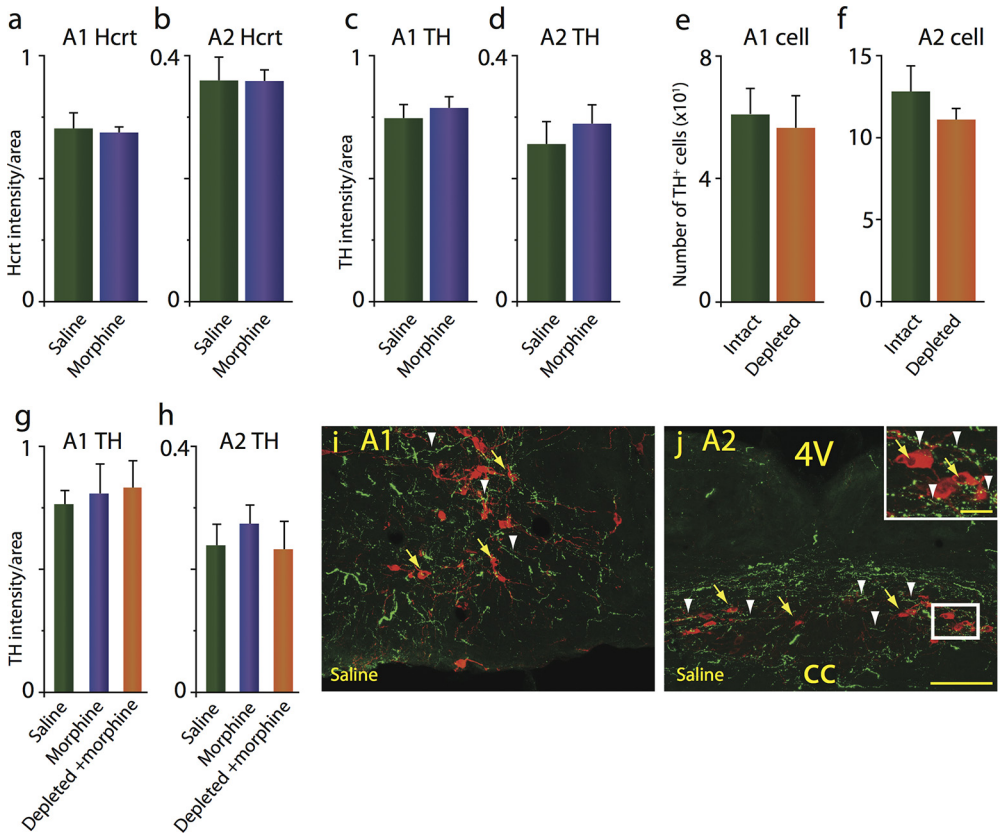

Figure 3. Morphine treatment does not alter Hcrt axon density, TH levels, or TH cell numbers in the A1/A2 medullary norepinephrine-containing regions. ***a***, ***b***, Intact-DTA-Hcrt animals treated with morphine (14 d, 50 mg/kg) did not show a significant change in Hcrt axonal labeling in the A1 (***a***) and the A2 (***b***) regions. ***c***, ***d***, TH levels remained comparable to baseline levels after morphine treatment in the A1 (***c***) and A2 (***d***) regions. ***e***, ***f***, TH^+ cell counts were unaffected by the elimination of Hcrt neurons in depleted-DTA-Hcrt animals in the A1 (***e***) or the A2 (***f***) regions. ***g***, ***h***, Deletion of Hcrt neurons did not affect TH levels in the A1 (***g***) and the A2 (***h***) regions after morphine treatment compared with intact-DTA-Hcrt animals treated with saline or morphine. ***i***, ***j***, Confocal images of representative sections of the A1 (***i***) and A2 (***j***) of an intact-DTA-Hcrt animal after saline treatment, illustrating the distribution of Hcrt fibers in green (white arrowheads) and TH^+ neurons in red (yellow arrows). Insert in ***j*** shows a higher magnification of white square. Scale bars: 100 μm; insert, 20 μm. cc, Central canal; 4V, fourth ventricle. $n = 4$/condition.

1997; Mazei-Robison and Nestler, 2012; Solecki et al., 2019). In addition, we observed that morphine treatment induced a significant increase in the levels of the TH enzyme, the rate-limiting step in the synthesis of NE (Kobayashi and Nagatsu, 2005) in this structure, and that this increase is entirely dependent on Hcrt. In contrast, we observed that Hcrt innervation and TH levels in the A1 and A2 medullary NE regions, structures also reported to affect opioid withdrawal behaviors (Delfs et al., 2000), were unaffected by morphine treatment.

In the current studies, we found that mice lacking Hcrt neurons (DTA-depleted) did not develop sensitization to repeated doses of morphine and displayed a reduction in the somatic and affective symptoms of withdrawal following naloxone administration in dependent animals.

Morphine exposure results in an increased Hcrt axon density in the LC but not in the A1 and A2 medullary regions

The increase in the number of detectable Hcrt neurons in the hypothalamus we have previously reported after morphine exposure is the result of augmented Hcrt peptide production in neurons that were not producing detectable levels of Hcrt under baseline conditions, not neurogenesis (McGregor et al., 2017; Thannickal et al., 2018). We now show that this increment in Hcrt peptide production is correlated with a significant increase in the number of detectable Hcrt axons in the LC, the brainstem structure receiving the largest Hcrt projections under baseline conditions (Peyron et al., 1998; Puskás et al., 2010). Most likely, Hcrt axons are present in the LC, but remain undetectable under baseline conditions. However, we cannot dismiss the possibility that axonal growth occurs as a result of morphine treatment.

On the other hand, the A1/A2 medullary regions, which also receive dense Hcrt projections (Puskás et al., 2010), did not show a significant increase in the level of Hcrt axonal presence after morphine treatment of intact-DTA-Hcrt mice, indicating that the increase in Hcrt innervation is region specific. Prior work has reported that disruption of A1/A2 NE transmission reduces only the affective component of opioid withdrawal (Delfs et al., 2000). In the present report, we show that the disruption of Hcrt transmission results in the reduction of both physical and affective symptoms of opioid withdrawal, suggesting a possible synergistic participation of the LC and A1/A2 in the opiate withdrawal syndrome.

The presence of Hcrt in the LC is necessary for the increase in the levels of TH in this structure after chronic opiate administration, since depletion of Hcrt neurons completely eliminated this change. A previous study reported that brain-derived neurotrophic factor from outside the LC is also critical for the increase in TH levels seen in this structure after morphine exposure (Akbarian et al., 2002). In contrast to the robust increase in the number of detected Hcrt neurons after opioid (Thannickal et al., 2018) or cocaine (James et al., 2019) administration, we do not see an increase in the number of TH^+ neurons in the LC or A1/A2 regions after opiate administration.

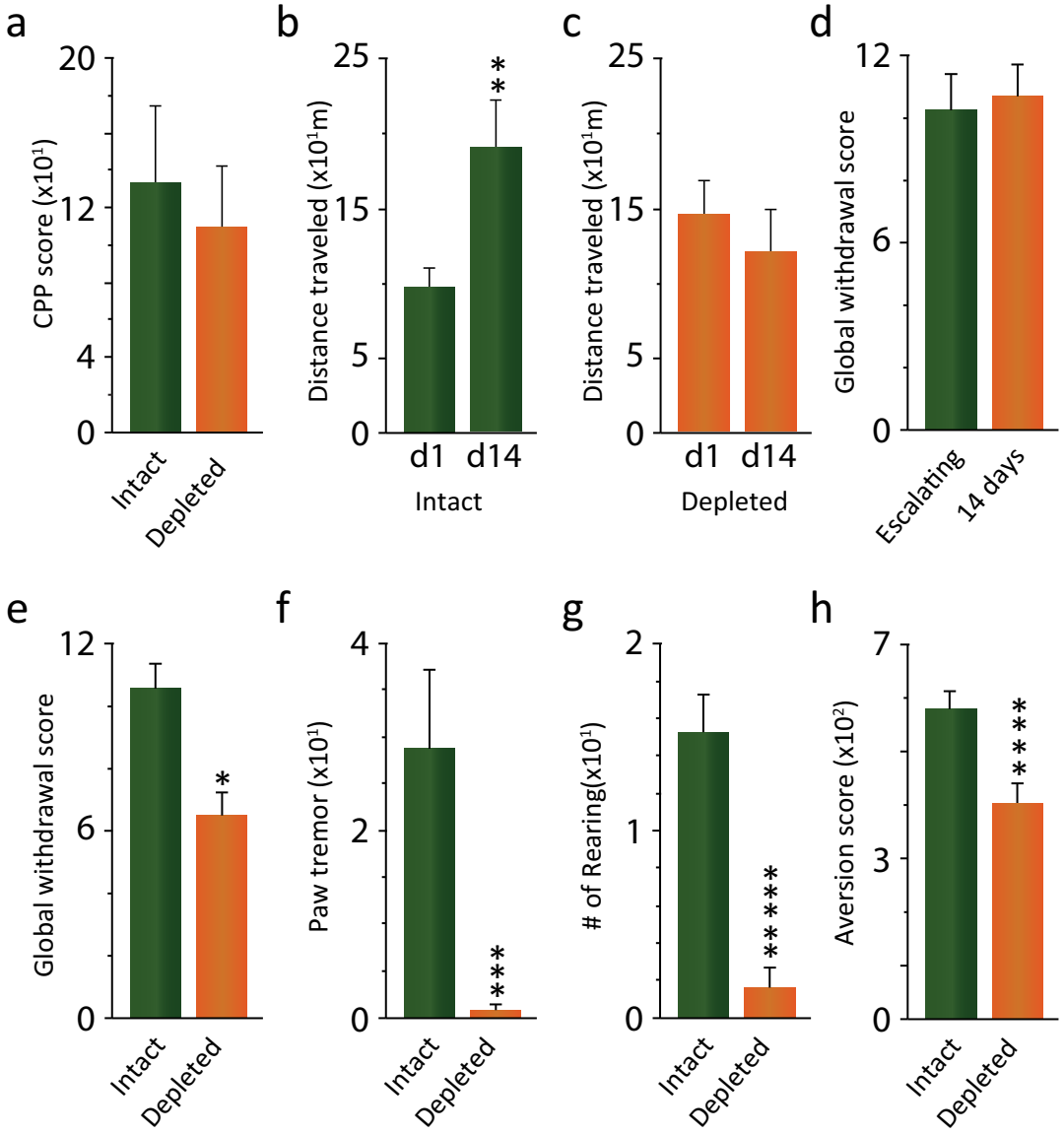

Figure 4. The rewarding properties of morphine are not significantly affected by the lack of Hcrt neurons. But Hcrt depletion prevents locomotor sensitization and reduces both the somatic signs of naloxone-precipitated withdrawal and naloxone conditioned place aversion in morphine-dependent animals. ***a***, Preference for the chamber paired with morphine did not significantly differ between intact-DTA-Hcrt and depleted-DTA-Hcrt animals ($n = 12$/condition). ***b***, Intact-DTA-Hcrt animals developed sensitization to repeated doses of morphine ($n = 6$). ***c***, Depletion of Hcrt neurons completely eliminated this addiction-linked behavior ($n = 6$). ***d***, Five days of escalating morphine and 14 d daily 50 mg/kg morphine doses resulted in comparable global symptom withdrawal scores ($n = 6$/condition). ***e***, Elimination of Hcrt neurons in depleted-DTA-Hcrt animals resulted in a significant reduction in the global withdrawal score compared with intact-DTA-Hcrt animals. ***f***, ***g***, Paw tremor (***f***) and rearing (***g***) showed the largest reduction of the somatic withdrawal signs ($n = 6$/condition). ***h***, Lack of Hcrt neurons significantly reduced the aversion to the chamber paired with naloxone ($n = 10$/condition). *****$p = 0.0001$, ****$p = 0.002$, ***$p = 0.007$, **$p = 0.04$, *$p = 0.043$.

Hcrt neurons, opiate reward, physical withdrawal, and conditioned aversion to opiate receptor blockade

In the current study, consistent with prior reports in Hcrt peptide knock-out mice, in which the Hcrt peptide is eliminated but the neurons remain (Sharf et al., 2010), we observed that mice in which Hcrt neurons were eliminated (depleted-DTA-Hcrt) develop a preference for the chamber previously paired with morphine at the same rate as intact-DTA-Hcrt animals, indicating that the lack of Hcrt neurons does not affect the rewarding properties of morphine. On the other hand, elimination of Hcrt neurons completely blocked locomotor sensitization to repeated doses of morphine, a response that develops in intact animals repeatedly exposed to morphine. This is in agreement with prior studies using a dual Hcrt receptor antagonist to block Hcrt transmission (Georgescu et al., 2003; Sharf et al., 2008; Laorden et al., 2012). Drug sensitization may correlate with the enhanced pleasure experienced by addicts with repeated drug injections (Robinson and Berridge, 1993; Kalivas and Volkow, 2005; Chefer and Shippenberg, 2009; Berridge and Kringelbach, 2013). The absence of this behavior in animals lacking Hcrt neurons parallels the finding in human narcoleptic patients, characterized by an average loss of 90% of Hcrt neurons (Thannickal et al., 2000), who show little, if any, evidence of drug abuse and addiction (Borgland et al., 2009; Brown and Guilleminault, 2011; Guilleminault and Fromherz, 2011; James et al., 2017), despite their daily prescribed use of γ-hydroxybutyrate (GHB), methylphenidate, and amphetamine, drugs frequently abused in the general population (Harris et al., 2007; Borgland et al., 2009;

Nishino and Mignot, 2011; Dauvilliers et al., 2013; Barateau et al., 2016; Jalal et al., 2018; Turner et al., 2018; Darke et al., 2019). Dose escalation and overdose are virtually nonexistent in narcoleptic patients (Galloway et al., 1997; Aston-Jones et al., 2010; Bayard and Dauvilliers, 2013; Baimel et al., 2015). Also, narcoleptics do not experience withdrawal when they take "drug holidays," from prescribed amphetamines or GHB (Brown and Guilleminault, 2011; Cao and Guilleminault, 2011). In addition, consistent with this and with prior animal studies (Georgescu et al., 2003; Sharf et al., 2008; Laorden et al., 2012), we observed that Hcrt-depleted mice displayed both a dampened physical response to naloxone-precipitated withdrawal when morphine dependent, and a lack of a CPA to a low dose of naloxone that does not precipitate physical withdrawal, indicating that the Hcrt system is involved in the modulation of both physical and affective components of withdrawal.

These results suggest that part of the mechanisms underlying the behavioral difference in response to naloxone withdrawal between intact-DTA-Hcrt and depleted-DTA-Hcrt morphine-dependent animals can be found in the lack of TH increase in the LC in animals lacking Hcrt neurons. Since TH is the rate-limiting step in the synthesis of NE (Kumer and Vrana, 1996), we hypothesize that the upregulation of this enzyme observed in animals with a full contingent of Hcrt neurons (intact-DTA-Hcrt) may increase the capacity of these neurons to produce NE, which in turn may lead to changes in the amounts of neurotransmitter released in the terminal fields. Because of the extensive projections of the LC throughout the neuraxis, altered NE levels in target regions may significantly impact the physiology of a plethora of systems, including those that regulate arousal, anxiety, and stress (Berridge and Waterhouse, 2003; Ross and Van Bockstaele, 2020), contributing to the effects of opioid withdrawal.

Together, the results of the current study open new possibilities for the treatment of opioid withdrawal through pharmacological modulation of the Hcrt system.

References

Akbarian S, Rios M, Liu RJ, Gold SJ, Fong HF, Zeiler S, Coppola V, Tessarollo L, Jones KR, Nestler EJ, Aghajanian GK, Jaenisch R (2002) Brain-derived neurotrophic factor is essential for opiate-induced plasticity of noradrenergic neurons. J Neurosci 22:4153–4162.

Aston-Jones G, Smith RJ, Sartor GC, Moorman DE, Massi L, Tahsili-Fahadan P, Richardson KA (2010) Lateral hypothalamic orexin/hypocretin neurons: a role in reward-seeking and addiction. Brain Res 1314:74–90.

Baimel C, Bartlett SE, Chiou LC, Lawrence AJ, Muschamp JW, Patkar O, Tung LW, Borgland SL (2015) Orexin/hypocretin role in reward: implications for opioid and other addictions. Br J Pharmacol 172:334–348.

Barateau L, Jaussent I, Lopez R, Boutrel B, Leu-Semenescu S, Arnulf I, Dauvilliers Y (2016) Smoking, alcohol, drug use, abuse and dependence in narcolepsy and idiopathic hypersomnia: a case-control study. Sleep 39:573–580.

Bayard S, Dauvilliers YA (2013) Reward-based behaviors and emotional processing in human with narcolepsy-cataplexy. Front Behav Neurosci 7:50.

Benturquia N, Le Guen S, Canestrelli C, Lagente V, Apiou G, Roques BP, Noble F (2007) Specific blockade of morphine- and cocaine-induced reinforcing effects in conditioned place preference by nitrous oxide in mice. Neuroscience 149:477–486.

Berridge CW, Waterhouse BD (2003) The locus coeruleus-noradrenergic system: modulation of behavioral state and state-dependent cognitive processes. Brain Res Brain Res Rev 42:33–84.

Berridge KC, Kringelbach ML (2013) Neuroscience of affect: brain mechanisms of pleasure and displeasure. Curr Opin Neurobiol 23:294–303.

Blanco-Centurion C, Gerashchenko D, Shiromani PJ (2007) Effects of saporin-induced lesions of three arousal populations on daily levels of sleep and wake. J Neurosci 27:14041–14048.

Blouin AM, Fried I, Wilson CL, Staba RJ, Behnke EJ, Lam HA, Maidment NT, Karlsson KAE, Lapierre JL, Siegel JM (2013) Human hypocretin and melanin-concentrating hormone levels are linked to emotion and social interaction. Nat Commun 4:1547.

Borgland SL, Chang SJ, Bowers MS, Thompson JL, Vittoz N, Floresco SB, Chou J, Chen BT, Bonci A (2009) Orexin A/hypocretin-1 selectively promotes motivation for positive reinforcers. J Neurosci 29:11215–11225.

Boutrel B, de Lecea L (2008) Addiction and arousal: the hypocretin connection. Physiol Behav 93:947–951.

Brown MA, Guilleminault C (2011) A review of sodium oxybate and baclofen in the treatment of sleep disorders. Curr Pharm Des 17:1430–1435.

Cao MT, Guilleminault C (2011) Narcolepsy: Diagnosis and management. In: In principles and practice of sleep medicine (Kryger MH RT, Dement WC, ed), pp 957–968. Missouri: Elsevier Saunders.

Chaijale NN, Curtis AL, Wood SK, Zhang XY, Bhatnagar S, Reyes BA, Van Bockstaele EJ, Valentino RJ (2013) Social stress engages opioid regulation of locus coeruleus norepinephrine neurons and induces a state of cellular and physical opiate dependence. Neuropsychopharmacology 38:1833–1843.

Chefer VI, Shippenberg TS (2009) Augmentation of morphine-induced sensitization but reduction in morphine tolerance and reward in delta-opioid receptor knockout mice. Neuropsychopharmacology 34:887–898.

Christie MJ, Williams JT, Osborne PB, Bellchambers CE (1997) Where is the locus in opioid withdrawal? Trends Pharmacol Sci 18:134–140.

Darke S, Kaye S, Duflou J, Lappin J (2019) Completed suicide among methamphetamine users: a national study. Suicide Life Threat Behav 49:328–337.

Dauvilliers Y, Lopez R, Ohayon M, Bayard S (2013) Hypersomnia and depressive symptoms: methodological and clinical aspects. BMC Med 11:78.

Delfs JM, Zhu Y, Druhan JP, Aston-Jones G (2000) Noradrenaline in the ventral forebrain is critical for opiate withdrawal-induced aversion. Nature 403:430–434.

Donjacour C, Lammers GJ, Siegel JM (2019) Striking cessation of cataplexy by opioids. J Sleep Res 28:e12781.

Fox ME, Bucher ES, Johnson JA, Wightman RM (2016) Medullary norepinephrine projections release norepinephrine into the contralateral bed nucleus of the stria terminalis. ACS Chem Neurosci 7:1681–1689.

Galloway GP, Frederick SL, Staggers FE Jr, Gonzales M, Stalcup SA, Smith DE (1997) Gamma-hydroxybutyrate: an emerging drug of abuse that causes physical dependence. Addiction 92:89–96.

Georgescu D, Zachariou V, Barrot M, Mieda M, Willie JT, Eisch AJ, Yanagisawa M, Nestler EJ, DiLeone RJ (2003) Involvement of the lateral hypothalamic peptide orexin in morphine dependence and withdrawal. J Neurosci 23:3106–3111.

Guilleminault C, Fromherz S (2011) Narcolepsy: diagnosis and management. In: Principles and practice of sleep medicine (Kryger MH, Roth RT, Dement WC, eds), pp 957–968. St. Louis, MO: Elsevier Saunders.

Harris GC, Wimmer M, Aston-Jones G (2005) A role for lateral hypothalamic orexin neurons in reward seeking. Nature 437:556–559.

Harris GC, Wimmer M, Randall-Thompson JF, Aston-Jones G (2007) Lateral hypothalamic orexin neurons are critically involved in learning to associate an environment with morphine reward. Behav Brain Res 183:43–51.

Hewitt BM, Yap MH, Hodson-Tole EF, Kennerley AJ, Sharp PS, Grant RA (2018) A novel automated rodent tracker (ART), demonstrated in a mouse model of amyotrophic lateral sclerosis. J Neurosci Methods 300:147–156.

Jalal H, Buchanich JM, Roberts MS, Balmert LC, Zhang K, Burke DS (2018) Changing dynamics of the drug overdose epidemic in the United States from 1979 through 2016. Science 361:eaau1184.

James MH, Mahler SV, Moorman DE, Aston-Jones G (2017) A decade of orexin/hypocretin and addiction: where are we now? Curr Top Behav Neurosci 33:247–281.

James MH, Stopper CM, Zimmer BA, Koll NE, Bowrey HE, Aston-Jones G (2019) Increased number and activity of a lateral subpopulation of hypothalamic orexin/hypocretin neurons underlies the expression of an addicted state in rats. Biol Psychiatry 85:925–935.

Jaremko KM, Thompson NL Jr, Reyes BA, Jin J, Ebersole B, Jenney CB, Grigson PS, Levenson R, Berrettini WH, Van Bockstaele EJ (2014) Morphine-induced trafficking of a mu-opioid receptor interacting

protein in rat locus coeruleus neurons. Prog Neuropsychopharmacol Biol Psychiatry 50:53–65.
John J, Thannickal TC, McGregor R, Ramanathan L, Ohtsu H, Nishino S, Sakai N, Yamanaka A, Stone C, Cornford M, Siegel JM (2013) Greatly increased numbers of histamine cells in human narcolepsy with cataplexy. Ann Neurol 74:786–793.
Kaeidi A, Azizi H, Javan M, Ahmadi Soleimani SM, Fathollahi Y, Semnanian S (2015) Direct facilitatory role of paragigantocellularis neurons in opiate withdrawal-induced hyperactivity of rat locus coeruleus neurons: an in vitro study. PLoS One 10:e0134873.
Kalivas PW, Volkow ND (2005) The neural basis of addiction: a pathology of motivation and choice. Am J Psychiatry 162:1403–1413.
Kobayashi K, Nagatsu T (2005) Molecular genetics of tyrosine 3-monooxygenase and inherited diseases. Biochem Biophys Res Commun 338:267–270.
Kumer SC, Vrana KE (1996) Intricate regulation of tyrosine hydroxylase activity and gene expression. J Neurochem 67:443–462.
Laorden ML, Ferenczi S, Pinter-Kubler B, Gonzalez-Martin LL, Lasheras MC, Kovacs KJ, Milanés MV, Nunez C (2012) Hypothalamic orexin–a neurons are involved in the response of the brain stress system to morphine withdrawal. PLoS One 7:e36871.
Maldonado R, Blendy JA, Tzavara E, Gass P, Roques BP, Hanoune J, Schutz G (1996) Reduction of morphine abstinence in mice with a mutation in the gene encoding CREB. Science 273:657–659.
Mazei-Robison MS, Nestler EJ (2012) Opiate-induced molecular and cellular plasticity of ventral tegmental area and locus coeruleus catecholamine neurons. Cold Spring Harb Perspect Med 2:a012070.
McGregor R, Wu MF, Barber G, Ramanathan L, Siegel JM (2011) Highly specific role of hypocretin (orexin) neurons: differential activation as a function of diurnal phase, operant reinforcement versus operant avoidance and light level. J Neurosci 31:15455–15467.
McGregor R, Shan L, Wu MF, Siegel JM (2017) Diurnal fluctuation in the number of hypocretin/orexin and histamine producing: implication for understanding and treating neuronal loss. PLoS One 12:e0178573.
Mileykovskiy BY, Kiyashchenko LI, Siegel JM (2005) Behavioral correlates of activity in identified hypocretin/orexin neurons. Neuron 46:787–798.
Nestler EJ (2013) Cellular basis of memory for addiction. Dialogues Clin Neurosci 15:431–443.
Nestler EJ, Barrot M, DiLeone RJ, Eisch AJ, Gold SJ, Monteggia LM (2002) Neurobiology of depression. Neuron 34:13–25.
Nishino S, Mignot E (2011) Narcolepsy and cataplexy. Handb Clin Neurol 99:783–814.
Parkitna JR, Solecki W, Gołembiowska K, Tokarski K, Kubik J, Gołda S, Novak M, Parlato R, Hess G, Sprengel R, Przewłocki R (2012) Glutamate input to noradrenergic neurons plays an essential role in the development of morphine dependence and psychomotor sensitization. Int J Neuropsychopharmacol 15:1457–1471.
Peyron C, Tighe DK, van den Pol AN, de Lecea L, Heller HC, Sutcliffe JG, Kilduff TS (1998) Neurons containing hypocretin (orexin) project to multiple neuronal systems. J Neurosci 18:9996–10015.
Prus AJ, James JR, Rosecrans JA (2009) Conditioned Place Preference. In: Methods of Behavior Analysis in Neuroscience, 2 Edition (JJB, ed). Chapter 4 pp 1–12 . Boca Raton, (FL) : CRC Press/Taylor and Francis.
Puskás N, Papp RS, Gallatz K, Palkovits M (2010) Interactions between orexin-immunoreactive fibers and adrenaline or noradrenaline-expressing neurons of the lower brainstem in rats and mice. Peptides 31:1589–1597.
Robinson TE, Berridge KC (1993) The neural basis of drug craving: an incentive-sensitization theory of addiction. Brain Res Brain Res Rev 18:247–291.
Ross JA, Van Bockstaele EJ (2020) The locus coeruleus-norepinephrine system in stress and arousal: unraveling historical, current, and future perspectives. Front Psychiatry 11:601519.
Sharf R, Sarhan M, Dileone RJ (2008) Orexin mediates the expression of precipitated morphine withdrawal and concurrent activation of the nucleus accumbens shell. Biol Psychiatry 64:175–183.
Sharf R, Guarnieri DJ, Taylor JR, DiLeone RJ (2010) Orexin mediates morphine place preference, but not morphine-induced hyperactivity or sensitization. Brain Res 1317:24–32.
Solecki WB, Kus N, Gralec K, Klasa A, Pradel K, Przewłocki R (2019) Noradrenergic and corticosteroid receptors regulate somatic and motivational symptoms of morphine withdrawal. Behav Brain Res 360:146–157.
Tabuchi S, Tsunematsu T, Black SW, Tominaga M, Maruyama M, Takagi K, Minokoshi Y, Sakurai T, Kilduff TS, Yamanaka A (2014) Conditional ablation of orexin/hypocretin neurons: a new mouse model for the study of narcolepsy and orexin system function. J Neurosci 34:6495–6509.
Thannickal TC, Moore RY, Nienhuis R, Ramanathan L, Gulyani S, Aldrich M, Cornford M, Siegel JM (2000) Reduced number of hypocretin neurons in human narcolepsy. Neuron 27:469–474.
Thannickal TC, John J, Shan L, Swaab DF, Wu MF, Ramanathan L, McGregor R, Chew KT, Cornford M, Yamanaka A, Inutsuka A, Fronczek R, Lammers GJ, Worley PF, Siegel JM (2018) Opiates increase the number of hypocretin-producing cells in human and mouse brain and reverse cataplexy in a mouse model of narcolepsy. Sci Transl Med 10: eaao4953.
Turner C, Chandrakumar D, Rowe C, Santos GM, Riley ED, Coffin PO (2018) Cross-sectional cause of death comparisons for stimulant and opioid mortality in San Francisco, 2005-2015. Drug Alcohol Depend 185:305–312.
Valentino RJ, Van Bockstaele E (2008) Convergent regulation of locus coeruleus activity as an adaptive response to stress. Eur J Pharmacol 583:194–203.
Wu MF, Nienhuis R, Maidment N, Lam HA, Siegel JM (2011a) Cerebrospinal fluid hypocretin (orexin) levels are elevated by play but are not raised by exercise and its associated heart rate, blood pressure, respiration or body temperature changes. Arch Ital Biol 149:492–498.
Wu MF, Nienhuis R, Maidment N, Lam HA, Siegel JM (2011b) Role of the hypocretin (orexin) receptor 2 (Hcrt-r2) in the regulation of hypocretin level and cataplexy. J Neurosci 31:6305–6310.
Zhang L, Kibaly C, Wang YJ, Xu C, Song KY, McGarrah PW, Loh HH, Liu JG, Law PY (2017) Src-dependent phosphorylation of μ-opioid receptor at Tyr(336) modulates opiate withdrawal. EMBO Mol Med 9:1521–1536.
Zhang Q, Liu Q, Li T, Liu Y, Wang L, Zhang Z, Liu H, Hu M, Qiao Y, Niu H (2016) Expression and colocalization of NMDA receptor and FosB/ΔFosB in sensitive brain regions in rats after chronic morphine exposure. Neurosci Lett 614:70–76.